17th World Conference on Earthquake Engineering, 17WCEE
Sendai, Japan - September 13th to 18th 2020

NONLINEAR RESPONSE OF BRIDGE PYLONS TO SURFACE WAVE PASSAGE

C. T. Chatzigogos[(1)], K. C. Meza-Fajardo[(2)], A. S. Papageorgiou[(3)]

[(1)] *Research Engineer, Géodynamique & Structure (France), charisis.chatzigogos@geodynamique.com*
[(2)] *Researcher, BRGM (France), k.mezafajardo@brgm.fr*
[(3)] *Professor, University of Patras (Greece), a.socrates.papageorgiou@gmail.com*

Abstract

One of the less well-understood aspects of the effects of earthquakes on civil structures is related to the generation (especially in sedimentary basins) of surface waves together with their subsequent impact on buildings and infrastructure. Surface waves are typically characterized by rich low-frequency content and long durations and accordingly they can be particularly damaging for long-period structures, such as high-rise buildings, bridge pylons, liquid storage tanks, telecommunication masts, water towers *etc*. The present paper proposes a concise surrogate mechanical model for the study of the seismic nonlinear response of bridge pylons. The model is fully parametrizable based on a reduced number of dimensionless parameters that allow generating easily different structural and foundation configurations. The model couples a multi-fiber beam model for the bridge pylon with a nonlinear macroelement for the pylon foundation accounting for sliding, uplift and partial or full loss of bearing capacity in the soil domain. The surrogate model is used for studying several characteristic pylon configurations by changing the main characteristics of the pylon and the foundation. The selected configurations are subjected to seismic signals, with and without the presence of the surface wave component (for horizontal translation and rotation). This allows identifying the effects of surface waves on the pylon and the foundation responses both in linear and in nonlinear regime and also helps quantifying the additional seismic demand induced by the presence of surface waves with reference to some relevant performance criteria for the bridge pylon and the foundation.

Keywords: bridge pylon design; surface waves; nonlinear soil-structure interaction; surrogate models

1. Introduction

In conventional seismic studies of civil engineering structures, it is customary to use incident motions obtained from 1D site response analyses. This approach leads to signals, which are devoid of the effect of surface waves that are generated in real geological/geotechnical settings, especially in the case of sedimentary basins. Neglecting the effect of surface waves is mainly justified by the fact that these waves exhibit low-frequency content ($\leq$ 1Hz) and as such, their impact is considered negligible for civil engineering structures, typically characterized by higher frequencies.

Nonetheless, several recent large earthquakes (Chi-Chi 1999, Chuetsu 2004, El Mayor 2010, Tohoku 2011) have revealed that long-period ground excitations related to the passage of surface waves and giving rise to significant incident rotational motions may be detrimental for long-period structures such as high-rise buildings, bridge pylons, liquid storage tanks, water towers, telecommunication masts *etc*. In two recent papers, Meza & Papageorgiou [1], [2], have proposed an efficient surrogate model for the study of large-period high-rise buildings (with fundamental period T_0 typically $\geq$ 1sec) under the effect of base rocking induced by Rayleigh waves. In the same context, the French research project ANR MODULATE (https://modulate.brgm.fr/, 2018-2022) focuses on the study of several types of long-period structures subjected to the effects of surface waves.

The present paper intends to extend the methodology proposed by Meza & Papageorgiou [1], [2] for high-rise buildings to the case of bridge pylons. To this end, a concise surrogate model for a typical pylon-

foundation system is proposed. This model is used for studying several characteristic pylon configurations placing the nonlinear response either on the superstructure or on the foundation. The seismic response of these configurations is studied for selected seismic records, which preserve at will the surface wave component for horizontal translation and rotation (rocking). These analyses allow quantifying the increase in seismic demand when the surface wave component is considered, and this, for a nonlinear response of either the superstructure or the foundation or of both.

2. Surrogate model for bridge pylons

Following the work by Meza & Papageorgiou [1], [2] for high-rise buildings, a surrogate model for a typical bridge pylon is herein proposed. The model is schematically presented on Fig. 1. Intended for studying the transverse dynamic response of a typical bridge pylon, the model is formulated in 2D kinematic conditions, with X designating the horizontal axis and Y the vertical axis (positive upwards). Notwithstanding the geometrical and architectural variants that may exist for a bridge pylon, the present model will refer to a single-branch bridge pier of uniform cross-section for its entire height. The pier supports at its top a portion of the bridge deck. The connection between the deck and the pier is concretized by a local spring-dashpot element. The pier is founded on the surface of the soil domain by means of a rigid footing. The embedment of the footing within the ground is neglected. For simplicity, the soil domain at the vicinity of the foundation can be considered homogeneous.

2.1 Mechanical modelling

The developed surrogate model is used for examining the seismic response of bridge pylons under the effect of surface waves. The basic constituents of the model are:

A) Consideration of the full nonlinear response of the pier in bending using multi-fiber beam elements. The pier is discretized into a number of 2-noded segmental beam elements. In 2D kinematics, each node is carrying three degrees of freedom ($\mathbf{u}^{\mathrm{T}} = \{u_X \ u_Y \ \theta_Z\}$). Additionally, the cross-section of the bridge pier is discretized into a number of "fibers", which are assigned an appropriate 1D nonlinear constitutive law depending on the materials of the pier. This model is thus capable of rigorously describing the nonlinear response of the bridge pier in bending. In the following, we adopt a simple elastoplastic law for all the fibers, characterized by an initial elastic stiffness E_p, a yield stress f_y and a post-elastic reduced stiffness $E_p' = \alpha_k E_p$ with α_k, a proportionality constant (*cf.* Fig. 1). Elastic stiffness E_p and yield stress f_y can be calibrated to provide a prescribed yield bending moment $M_{p,y}$ for a characteristic yield curvature κ_y of the pier section.

B) Consideration of the nonlinear response at the foundation level. To this end, we use the nonlinear foundation macroelement developed by Chatzigogos *et al*. [3]. This macroelement allows for the modeling of nonlinear mechanisms developing at the soil-foundation interface, namely the mechanisms of sliding, uplifting and soil plasticity. The model is concretized by a 2-noded spring element (the nodes can be placed on the same coordinates): the first node of the spring corresponds to the soil-footing interface; the second node is a control node, to which we apply boundary conditions or inject the seismic motions. The macroelement model is presented in further detail in §2.3.

C) Seismic excitation is characterized by a horizontal displacement time history $u_X(t)$ and a rotational time history $\theta_Z(t)$ which are applied as imposed displacements to the control node at the base of the model. In the present analyses, three scenarios of seismic motions are studied: 1) only horizontal excitation $u_X(t)$ exempt of the effect of surface waves, 2) only horizontal excitation, but with consideration of the surface wave contribution and 3) horizontal excitation $u_X(t)$ and rotational excitation $\theta_Z(t)$, both with consideration of the surface wave contribution. The vertical component of the excitation is not considered in the present analyses.

D) The resolution of the dynamic problem is performed in time domain using a Newmark unconditionally stable time integration scheme. The analyses can be performed under the assumption of either

small or large displacements (in the latter case, the model geometry is updated at each iteration). Calculations are run with open-source FEM platform Code_ASTER [4].

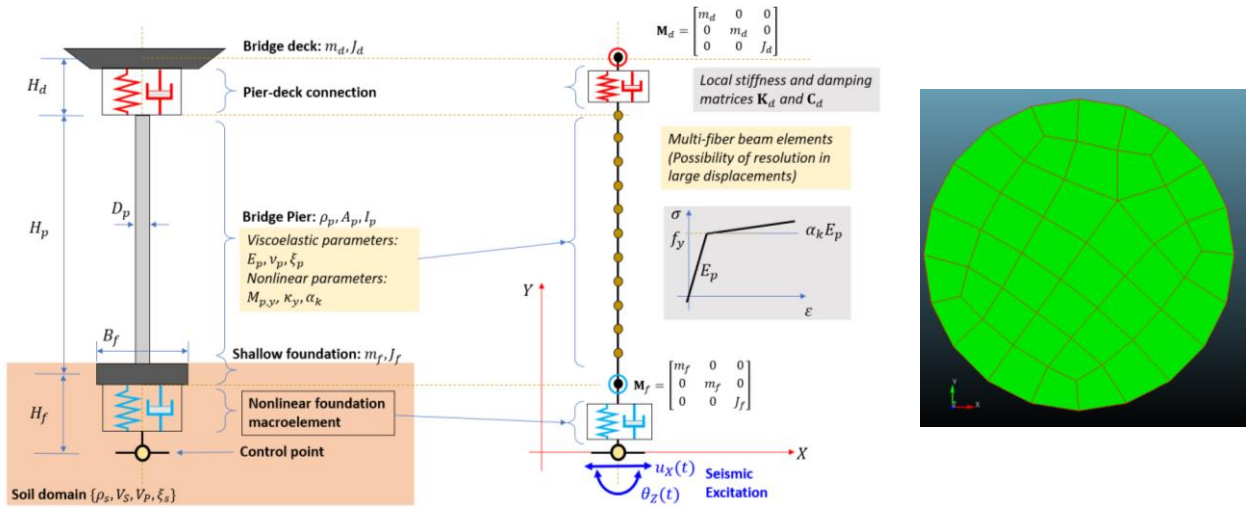

Fig. 1 –Surrogate model for bridge pylons and discretization of pier section in fibers

2.2 Geometric and mechanical characterization and dimensionless parameters

The surrogate model is defined by a number of geometrical and mechanical parameters and for convenience we can use subscripts d, p, f and s to designate respectively parameters pertaining to the deck, the pier, the foundation and the soil.

Geometric parameters. The main geometric parameter of the model is the height of the bridge pier H_p. The total height of the system can be obtained by adding to H_p, the foundation thickness H_f and the distance H_d between the center of gravity of the deck to the upper face of the bridge pier ($H_{\text{tot}} = H_d + H_p + H_f$). Two additional geometric parameters are necessary: the equivalent diameter of the bridge pier D_p (without loss of generality, we consider piers of circular cross-section) and the characteristic dimension of the foundation B_f (dimension in the transverse direction) (*cf.* Fig. 1).

Mass parameters. The bridge pier is characterized by a uniform cross section over its entire height. The mass of the pier is thus $m_p = \rho_p A_p H_p$, with ρ_p the mass density of the pier constitutive material (typically reinforced concrete with $\rho_p = 0.0025$kt/m^3) and A_p the cross-sectional area of the pier. For the deck and the foundation, we consider lumped diagonal mass matrices $\mathbf{M}_d$ and $\mathbf{M}_f$, in which we define the translation mass components m_d and m_f and also the corresponding rotational components (moments of inertia) J_d and J_f. The consideration of local moments of inertia for the foundation and the deck is deemed necessary since emphasis in given on the rotational component of the response.

Viscoelastic parameters. The model allows for the complete characterization of the nonlinear behavior in the pier-deck connection, the pier itself and at the foundation level via the nonlinear foundation macroelement. At first, it is necessary to define the linear elastic counterpart of these constitutive laws. For the pier-deck connection it is possible to consider local stiffness and damping matrices $\mathbf{K}_d$ and $\mathbf{C}_d$ corresponding to the adopted system of deck support (*e.g.* elastomeric bearings, isolators *etc.*) However, for convenience, it will be supposed in the following that the deck is rigidly connected to the pier head. For the bridge pier, we consider two elastic parameters of the pier constitutive material (Young's modulus E_p and Poisson's ratio ν_p) and a basic damping ratio ξ_p to be considered for the linear viscoelastic response of the pier. Beyond the yield moment threshold, material damping will be obtained via the adopted elastoplastic law of pier fibers. For the soil domain, and under the assumption of an approximately homogeneous profile at the pylon location, we

define mass density ρ_s, the "effective" elastic wave propagation velocities V_S (S-waves) and V_P (P-waves) and a basic damping ratio ξ_s for far-field material damping. These quantities, together with the shape of the foundation are used to determine the dynamic impedance functions of the foundation, which are complex and frequency-dependent and which are grouped within the foundation stiffness matrix $\mathbf{K}_f$ and damping matrix $\mathbf{C}_f$. The above parameters give rise to the main dynamic characteristics of the studied system, which are: a) the fixed-base fundamental period of the pier T_p and b) the fundamental period of the pier-foundation system T_{SSI} (pier with SSI).

Nonlinear parameters. As stated above, the basic nonlinear parameter for the pier bridge is yield moment $M_{p,y}$ and corresponding curvature κ_y. These two quantities are linked via the relationship: $M_{p,y} = E_p I_p \kappa_y$, with I_p, the moment of inertia of the pier section. Since the pier responds as a cantilever beam, yield moment $M_{p,y}$ will be developed at the lower section of the pier and will thus be in contrast with the overturning moment $M_{f,\max}$ that can be sustained by the foundation. Besides the maximum overturning moment $M_{f,\max}$, basic nonlinear parameters for the macroelement are the maximum central vertical force $N_{f,\max}$ and the maximum horizontal force $V_{f,\max}$ that can be sustained by the foundation.

Dimensionless parameters. For studying different variants of the presented surrogate model, it is more convenient to work with dimensionless parameters. In the following, dimensionless parameters will be designated with a tilde (~). We thus introduce the following definitions:

- Lengths are normalized with respect to the pier height H_p. This leads to the normalized foundation height $\tilde{H}_f = H_f/H_p$, the normalized foundation dimension $\tilde{B}_f = B_f/H_p$ *etc.*
- Mass parameters are normalized with respect to the mass of the pier m_p. This yields the normalized foundation mass $\tilde{m}_f = m_f/m_p$ and the normalized deck mass $\tilde{m}_d = m_d/m_p$. Mass densities can be normalized with respect to the mass density of the pier ρ_p.
- Moments on inertia are normalized with respect to the characteristic quantity $m_p H_p^2$. This leads to the normalized foundation rotational inertia $\tilde{J}_f = J_f/m_p H_p^2$ and the normalized deck rotational inertia $\tilde{J}_d = J_d/m_p H_p^2$.
- Forces are normalized with respect to the pier weight $W_p = m_p g$. The normalized maximum centered force at the foundation is $\mathrm{FS_{st}} = \tilde{N}_{f,\max} = N_{f,\max}/W_p$ (this quantity actually corresponds to the foundation safety factor $\mathrm{FS_{st}}$ for static loads). The normalized maximum horizontal force sustained by the foundation is $\tilde{V}_{f,\max} = V_{f,\max}/W_p$.
- Moments are normalized with respect to the pier yield moment $M_{p,y}$. For example, the normalized maximum moment sustained by the foundation is $\tilde{M}_{f,\max} = M_{f,\max}/M_{p,y}$
- Damping and Poisson's ratios are dimensionless by definition.
- Stress quantities can be normalized with respect to yield stress f_y or the Young's modulus E_p of pier fibers (depending on the context) and periods can be normalized with respect to the fixed-base period of the pier T_p.
- Finally, propagation velocities can be normalized with respect to characteristic quantity H_p/T_p. For instance, normalized soil shear wave velocity can be defined as $\tilde{V}_S = V_S T_p/H_p$. This quantity is an index of the rigidity contrast between the soil and the structure.

With the above definitions, each instance (configuration) of the surrogate model can be defined via the set of 5 main dimensional parameters:

$$\mathbf{a}^{\mathrm{T}} = \{H_p, m_p, E_p, T_p, M_{p,y}\} \tag{1}$$

and the following set of 17 dimensionless parameters:

$$\mathbf{b}^{\mathrm{T}} = \{\tilde{H}_d, \tilde{D}_p, \tilde{H}_f, \tilde{B}_f, \tilde{m}_d, \tilde{m}_f, \tilde{J}_d, \tilde{J}_f, \xi_p, \xi_s, \nu_p, \nu_s, \tilde{\rho}_s \tilde{V}_S, \tilde{N}_{f,\max}, \tilde{V}_{f,\max}, \tilde{M}_{f,\max}\} \tag{2}$$

2.3 Nonlinear foundation macroelement

The nonlinear foundation macroelement implemented in this study (*cf.* Chatzigogos et al. [3]) is an advanced link element placed at the base of the structure and reproducing the nonlinear response of the foundation under earthquake action. The basic constituents of the macroelement model are the following (all physical quantities refer to the foundation and we drop the index "f" for simplicity):

- The foundation is considered to be perfectly rigid: in 2D kinematics, any motion of the foundation is described by three degrees-of-freedom $\mathbf{u}^{\mathrm{T}} = \{u_X \;\; u_Y \;\; \theta_Z\}$ which give rise to the corresponding force parameters $\mathbf{Q}^{\mathrm{T}} = \{V \;\; N \;\; M\}$, where V, the horizontal force, N the vertical centered force and M, the overturning moment on the foundation. The macroelement provides a constitutive law for relating the increment of displacements $\dot{\mathbf{u}}$ to the corresponding increment of forces $\dot{\mathbf{Q}}$. The total displacement increment $\dot{\mathbf{u}}$ is decomposed into increments coming from the linear elastic counterpart of the macroelement constitutive law ($\dot{\mathbf{u}}_{\mathrm{lin}}$) and also from the nonlinear mechanisms that are considered within the macroelement, namely the uplift mechanism ($\dot{\mathbf{u}}_{\mathrm{up}}$), the sliding mechanism ($\dot{\mathbf{u}}_{\mathrm{sl}}$) and the soil plasticity mechanism ($\dot{\mathbf{u}}_{\mathrm{sp}}$). The total displacement increment thus reads:

$$\dot{\mathbf{u}} = \dot{\mathbf{u}}_{\mathrm{lin}} + \dot{\mathbf{u}}_{\mathrm{up}} + \dot{\mathbf{u}}_{\mathrm{sl}} + \dot{\mathbf{u}}_{\mathrm{sp}} \tag{3}$$

- In the linear case ($\dot{\mathbf{u}}_{\mathrm{lin}}$), the macroelement reproduces the dynamic impedance terms of the foundation. For a shallow foundation without embedment and for 2D kinematics, the impedance matrix is a 3×3 diagonal matrix with complex, frequency-dependent coefficients. In the present model, the frequency-dependence of the impedance terms may be dropped by selecting terms that correspond to the fundamental SSI period of the pier-foundation system. This then allows describing the viscoelastic linear part of macroelement law with three stiffness terms $\{K_{NN}, K_{VV}, K_{MM}\}$ and the corresponding damping terms $\{C_{NN}, C_{VV}, C_{MM}\}$. For simple foundation configurations, impedance terms can be calculated by charts and analytical expressions (*cf.* [5]).
- The uplift mechanism ($\dot{\mathbf{u}}_{\mathrm{up}}$) is a non-dissipative, reversible mechanism modeled via a nonlinear elastic law which couples the response between the vertical force N and the overturning moment M of a rigid foundation uplifting on the soil medium. The parameters governing this nonlinear elastic law only depend on the geometry of the foundation. Chatzigogos *et al.* [3] have proposed uplift models for strip or circular footings under planar loading conditions.
- The sliding mechanism ($\dot{\mathbf{u}}_{\mathrm{sl}}$) is a dissipative, non-reversible mechanism that depends on the soil-foundation interface strength criterion. For most practical applications, the interface strength is described by the Mohr-Coulomb criterion, characterized by the interface friction angle ϕ_{int} and the interface cohesion c_{int}. Moreover, a common assumption is to inherit strength properties from the soil in order to characterize the interface, so there is no distinction between the soil and the interface strength criteria.
- Finally, the plasticity mechanism ($\dot{\mathbf{u}}_{\mathrm{sp}}$) aims at describing the irreversible foundation behavior due to soil plasticity. This is achieved via a plasticity model which is equipped with an appropriately defined yield surface in the space of force parameters $\{N, V, M\}$. The form of this yield surface depends on the soil strength criterion and may be either ellipsoidal (centered at the origin) for a purely cohesive soil or rugby-ball shaped (with the origin lying on one of its two apices) for a purely frictional material or a combination of the two. In all cases, the yield surface can be adequately described by three parameters: a) the maximum centered vertical force $N_{f,\max}$, b) the maximum horizontal force $V_{f,\max}$ and c) the maximum overturning moment $M_{f,\max}$. Quantities $V_{f,\max}$ and $M_{f,\max}$ can be expressed by means of $N_{f,\max}$ and two dimensionless parameters ψ and χ as follows:

$$\psi = \frac{V_{f,\max}}{N_{f,\max}} \,|\, \chi = \frac{M_{f,\max}}{B_f N_{f,\max}} \tag{4}$$

- The plasticity model is completed with the definition of a hardening rule and a flow rule. For these definitions, the implemented macroelement follows the hypo-plasticity model with bounding surface proposed by Dafalias & Hermann [6]. In this formulation, the cyclic plastic modulus is written as follows:

$$\mathbf{H} = \frac{1}{h}\mathbf{n} \otimes \mathbf{n}_g \text{ with } h = h_0 \ln\left(\frac{\lambda^{p+1}}{\lambda_{\min}^{p}}\right) \tag{5}$$

Parameters h_0 and p are scalar quantities, λ is the distance between the current force state and an appropriately selected image point on the yield surface, and $\lambda_{\min}$ is the smallest value of λ recorded during cyclic (seismic) loading. Vectors $\mathbf{n}$ and $\mathbf{n}_g$ are normal vectors on the yield surface and the surface of plastic potential respectively and $\otimes$ designates the tensor product of two vectors. For simplicity, it is customary to define $\mathbf{n}_g$ by relating its elements to the vector $\mathbf{n}$ as follows:

$$\mathbf{n}_g^{\mathrm{T}} = \{p_g n_N \;\; n_V \;\; n_M\} \tag{6}$$

In other words, vector $\mathbf{n}_g$ is identical to $\mathbf{n}$ with the exception of the component parallel to the vertical force N, which is modified by the non-associative factor p_g. This parameter expresses the extent of vertical settlement of the foundation when subjected to load cycles under horizontal force or moment.

- Coupling among the different nonlinear mechanisms (in particular, uplift and soil plasticity) is achieved by an iterative procedure, in which all mechanisms must comply with the same force increment $\dot{\mathbf{Q}}$. Additionally, an *ad hoc* expression is introduced for defining the moment of uplift initiation M_{up} for an elastoplastic soil as a function of the vertical force N:

$$\frac{M_{\mathrm{up}}}{B_f} = \pm\frac{N}{a}e^{-\zeta\left(\frac{N}{N_{f,\max}}\right)} \tag{7}$$

with ζ, a numerical parameter varying between 1.5 and 2.5 and $\alpha = 4$ for strip footings.

3. Studied configurations

The configurations to be analyzed in the following are inspired from the pylons studied in [7]. In total, seven pylon configurations are studied. The characteristics of these configurations are summarized in Table 1. The basic scenario is a RC pier with height $H_p = 30$m and circular cross-section with $D_p = 3$m and a foundation with characteristic dimension $B_f = 11$m.

The yield moment of this pier is $M_{p,y} = 43$MNm for a corresponding curvature $\kappa_y = 3.6$E-4 [1/m]. For the pier fibers, we consider an equivalent yield stress $f_y = 16.22$MPa and a small hardening parameter $\alpha_k = 0.001$. Using this configuration as reference, we consider four variants of this pier with heights: 21m, 40m, 50m and 60m. All the other characteristics of the pier are preserved. Two additional configurations are obtained by reducing the foundation dimension to $B_f = 7.0$m for the piers with $H_p = 21$m and $H_p = 30$m. The configurations are designated for convenience "p21", "p30" *etc.* and "p21-RF" and "p30-RF" for the configurations with reduced foundation.

Table 1 provides some additional design parameters of the studied piers. The fundamental periods of vibration (with SSI) of the seven cases vary from $T_{\mathrm{SSI}} = 1.31$s for p21 to $T_{\mathrm{SSI}} = 6.11$s for p60. The safety factors of foundation design vary from $\mathrm{FS_{st}} = 2.35$ for p30-RF to $\mathrm{FS_{st}} = 5.19$ for p21. Finally, the minimal factor for elastic buckling is obtained for p60 and equals 2.91.

Soil conditions are identical for all studied configurations. The soil profile consists of a uniform stiff clay layer underlain by a rigid substratum. The parameters characterizing the soil profile are provided in Table 2(a). These quantities are necessary for determining the foundation impedance terms and the maximum centered vertical force $N_{f,\max}$ supported by the foundation. Table 2(b) summarizes the obtained foundation

impedance terms (for more details on the calculation of impedance terms, *cf.* [7]) and the numerical parameters for the implementation of foundation macro-elements following [3].

Table 1 – Geometrical and mechanical parameters of studied configurations

PHYSICAL QUANTITY	SYMBOL	UNIT	Pier 21 (p21)	Pier 21 (p21-RF)	Pier 30 (P30)	Pier 30 (p30-RF)	Pier 40 (p40)	Pier 50 (p50)	Pier 60 (p60)
Column height	H_p	[m]	21.0	21.0	30.0	30.0	40.0	50.0	60.0
Foundation characteristic dimension	B_f	[m]	11.0	7.0	11.0	7.0	11.0	11.0	11.0
Foundation height	H_f	[m]	2.0	2.0	2.0	2.0	2.0	2.0	2.0
Pier-deck connection height	H_d	[m]	0.0	0.0	0.0	0.0	0.0	0.0	0.0
Pier section diameter	D_p	[m]	3.0	3.0	3.0	3.0	3.0	3.0	3.0
Pier section radius	R_p	[m]	1.5	1.5	1.5	1.5	1.5	1.5	1.5
Pier cross-sectional area	A_p	[m²]	7.1	7.1	7.1	7.1	7.1	7.1	7.1
Pier cross section moment of inertia	I_p	[m⁴]	4.0	4.0	4.0	4.0	4.0	4.0	4.0
Mass density of the bridge pier	ρ_p	[kt/m³]	0.0025	0.0025	0.0025	0.0025	0.0025	0.0025	0.0025
Total mass of the pier	m_p	[kt]	0.371	0.371	0.530	0.530	0.707	0.884	1.060
Mass of the deck	m_d	[kt]	1.2	1.2	1.2	1.2	1.2	1.2	1.2
Moment of inertia of the deck	J_d	[ktm²]	23.4	23.4	23.4	23.4	23.4	23.4	23.4
Mass of the foundation	m_f	[kt]	0.605	0.245	0.605	0.245	0.605	0.605	0.605
Moment of inertia of the foundation	J_f	[ktm²]	4.777	0.832	4.777	0.832	4.777	4.777	4.777
Young modulus of pier	E_p	[MPa]	30000	30000	30000	30000	30000	30000	30000
Poisson's ratio of pier	ν_p	[-]	0.2	0.2	0.2	0.2	0.2	0.2	0.2
Basic damping ratio of pier	ξ_p	[%]	5.0	5.0	5.0	5.0	5.0	5.0	5.0
Yield moment of pier section	$M_{p,y}$	[MNm]	43.0	43.0	43.0	43.0	43.0	43.0	43.0
Yield curvature of pier section	$\kappa_{p,y}$	[1/m]	0.00036	0.00036	0.00036	0.00036	0.00036	0.00036	0.00036
Equivalent yield stress of pier fibers	f_y	[MPa]	16.22	16.22	16.22	16.22	16.22	16.22	16.22
Hardening parameter for pier fibers	α_k	[MPa]	0.001	0.001	0.001	0.001	0.001	0.001	0.001
Soil mass density	ρ_s	[kt/m³]	0.0016	0.0016	0.0016	0.0016	0.0016	0.0016	0.0016
Fundamental period (fixed-base conditions)	T_p	**[sec]**	**1.206**	**1.206**	**2.036**	**2.036**	**3.149**	**4.445**	**5.914**
Fundamental period of system with SSI	T_{SSI}	**[sec]**	**1.313**	**1.579**	**2.167**	**2.506**	**3.304**	**4.623**	**6.113**
Maximum centered vertical force at the foundation	$N_{f,\max}$	[MN]	110.81	45.52	110.81	45.52	110.81	110.81	110.81
Total weight of bridge pier	W_{tot}	[MN]	21.35	17.82	22.91	19.38	24.64	26.37	28.11
Load for elastic buckling	P_{crit}	[MN]	667.39	667.39	327.02	327.02	183.95	117.73	81.75
Minimal Factor of safety againgst elastic buckling	FS_b	[-]	31.26	37.46	14.28	16.88	7.47	4.46	2.91
Bearing capacity cactor of safety for static loads	FS_{st}	[-]	5.19	2.55	4.84	2.35	4.50	4.20	3.94

Table 2 – Parameters for: (a) soil profile and (b) foundation modeling with macroelement

(a)

Quantity	Symbol	Unit	Value
Soil mass density	ρ_s	[kt/m³]	0.0016
Soil Young's modulus (effective)	E_s	[MPa]	270.0
Soil Poisson's ratio	ν_s	[-]	0.3
Soil shear modulus (effective)	G_s	[MPa]	103.85
Soil shear wave velocity (effective)	V_S	[m/s]	254.8
Soil P-wave velocity (effective)	V_P	[m/s]	476.6
Basic damping ratio of soil	ξ_s	[%]	5.0
Lysmer's analog velocity	V_{La}	[m/s]	393.88
Soil layer depth	d_s	[m]	25.0
Soil cohesion	c_u	[MPa]	0.15

(b)

PARAMETER DESCRIPTION	SYMBOL	UNIT	Reduced	Basic
Footing dimension	B_f	[m]	7.00	11.00
Maximum centered vertical force	$N_{f,\max}$	[MN]	45.52	110.81
Maximum horizontal force	$V_{f,\max}$	[MN]	7.35	18.15
Maximum overturning moment	$M_{f,\max}$	[MNm]	34.47	133.77
Bounding surface parameter ψ	ψ	[-]	0.16	0.16
Bounding surface parameter ξ	χ	[-]	0.11	0.11
Footing elastic rigidity (vertical direction)	K_{NN}	[MN/m]	2577.32	4247.64
Footing elastic rigidity (horizontal direction)	K_{VV}	[MN/m]	2193.60	3688.98
Footing elastic rigidity (rotational direction)	K_{MM}	[MNm]	23443.05	92178.41
Footing dashpot coefficient (vertical direction)	A_{NN}	[MNs/m]	30.88	76.26
Footing dashpot coefficient (horizontal direction)	A_{VV}	[MNs/m]	2.20	5.43
Footing dashpot coefficient (rotation)	A_{MM}	[MNms]	0.00	0.00
Plastic parameter for virgin loading	h_0/K_{NN}	[-]	4.00	4.00
Plastic parameter for reloading	p	[-]	0.50	0.50
Non-associative parameter	p_g	[-]	5.00	5.00
Uplift initiation parameter (strip footing geometry)	α	[-]	4.00	4.00
Uplift parameter	γ	[-]	1.00	1.00
Uplift parameter	δ	[-]	1.00	1.00
Uplift parameter	ε	[-]	0.20	0.20
Uplift - plasticity coupling parameter	ζ	[-]	1.50	1.50

4. Definition of seismic motions

In studying high-rise buildings, Meza & Papageorgiou [1], [2] have considered a consistent set of 10 seismic motions in which it has been possible to extract the surface wave contribution in the horizontal and rotational

degrees-of-freedom. For the needs of the present analyses, only two records will be used, namely TKY018 and TCU140. The parameters pertaining to these records are presented in Table 3 together with the corresponding time histories.

Table 3 – Seismic motions considered in the analyses

	N/N	[-]	1	2
Record	Earthquake	[-]	Tohoku	Chi-Chi aftershock 1803
	Year	[-]	2011	1999
	Magnitude	M	9.0	6.2
	Depth	[km]	29	60
	Record Name	[-]	TKY018	TCU140
	Time Step	[dt]	0.040001646	0.035073000
	Nyquist frequency	[Hz]	12.50	14.26
	Scale Factor		1.00	4.79
Total Translation	Maximum Acceleration	[m/s2]	1.734750	0.362442
	Maximum Velocity	[m/s]	0.357248	0.162964
	Maximum Displacement	[m]	0.103189	0.132218
	Arias Intensity	[m/s]	2.013390	0.109693
	CAV	[m/s]	32.197	6.349
	Effective Duration	[s]	95.404	58.326
Translation (no SW)	Maximum Acceleration	[m/s2]	1.4249	0.314438
	Maximum Velocity	[m/s]	0.286039	0.0973062
	Maximum Displacement	[m]	0.0960181	0.0768128
	Arias Intensity	[m/s]	1.23489	0.0613608
	CAV	[m/s]	25.2619	4.72925
	Effective Duration	[s]	95.0839	61.8688
Total Rotation	Maximum Acceleration	[rad/s2]	0.00704208	0.00101921
	Maximum Velocity	[rad/s]	0.000246049	4.35912E-05
	Maximum Rotation	[rad]	2.58384E-05	3.17444E-05
	Arias Intensity	[rad/s]	1.56183E-05	1.36785E-07
	CAV	[rad/s]	0.0719398	0.0054708
	Effective Duration	[s]	44.8018	48.506

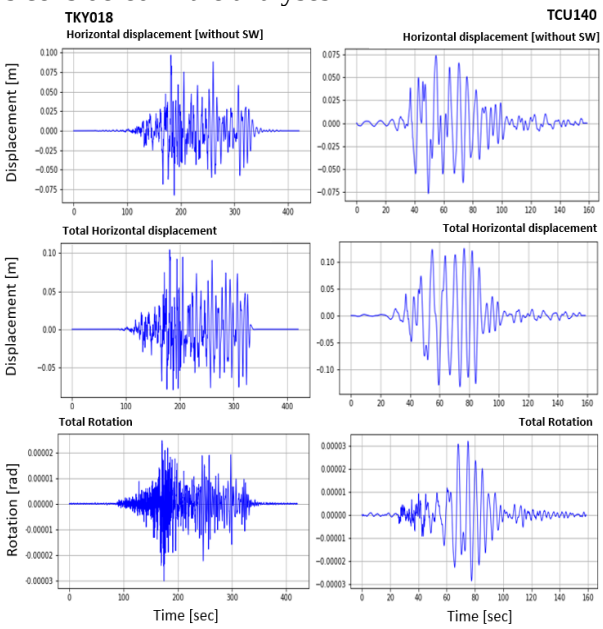

For each record, we retain three characteristic signals as shown in Table 3: a) the signal of horizontal translation without the effect of surface waves, b) the signal of total horizontal displacement, *i.e.* comprising the effect of surface waves and c) the signal of total rotation (comprising the effect of surface waves). These three signals allow performing three distinct scenarios of time history analyses:

- *Scenario* 1: Only signal a) is injected at the base of the pylon
- *Scenario* 2: Only signal b) is injected at the base of the pylon
- *Scenario* 3: Signals b) and c) are injected at the base of the pylon

The scenarios are defined in a hierarchical order, in which scenario 1 is totally exempt of any surface wave effect, scenario 2 introduces the effect encapsulated in the horizontal component and scenario 3, the total effect of both the horizontal and rotational components. Regarding the selected records, it can be noted that they have been defined with a relatively large time step dt and that they have particularly long durations. Record TCU140 presents relatively low accelerations and for this reason it has been scaled to the same acceleration as record TKY018, which is around 1.73m/s² so that the results of the two records can be comparable. Notice that Table 3 presents the unscaled properties of TCU140 and that the adopted scale factor is 4.79. Additionally, record TCU140 exhibits the strongest rotational component, which is nonetheless rather small, not exceeding 0.035mrad in the unscaled record and 4.79×0.035 = 0.17mrad in the scaled record.

5. Analysis results

5.1 General presentation of results

The above definitions for the pier configurations, the seismic motions and the scenarios of excitation result to a set of 42 nonlinear time-history analyses. The calculations are performed with software Code_ASTER [4] under the assumption of small displacements. The response for each case is probed by plotting 12 diagrams, organized in 4 rows and 3 columns as in Figs. 2 and 3. The columns correspond to the three examined scenarios of excitation (1: horizontal without SW effect / 2: horizontal with SW effect / 3: horizontal and rocking with SW effect). As for the rows, the first one presents the moment-curvature $\{M_p - \kappa\}$ diagram at the base of the

pylon. This diagram shows if the pier enters in nonlinear response and allows obtaining the ductility demand DD in the pier:

$$\mathrm{DD} = \max_{t}\left\{\frac{|\kappa(t)|}{\kappa_y}\right\} \tag{8}$$

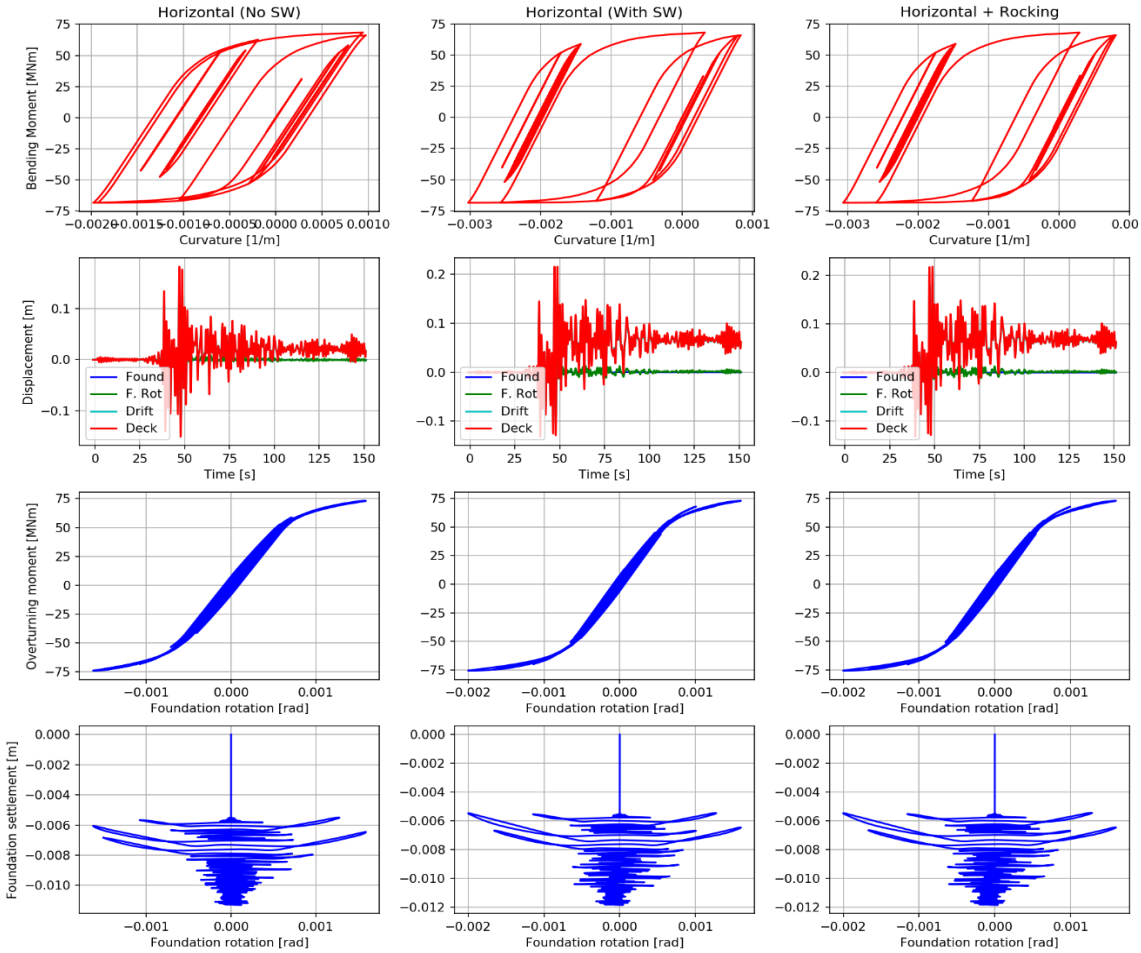

Fig. 2 – Response of p21 for record TCU140

The second row provides the evolution of the horizontal displacement at the deck of the pier, together with its three components: a) the horizontal displacement of the foundation, b) the horizontal displacement due to foundation rotation and c) the horizontal displacement due to structural drift. The third row provides the moment-rotation $\{M_f - \theta_Z\}$ diagram at the foundation level. Finally, the fourth diagram presents the evolution of foundation settlement plotted versus the foundation rotation.

The cases presented in Figs. 2 and 3 correspond respectively to p21 under record TCU140 and to p21-RF (reduced foundation) under the same record TCU140. In the first case (*cf.* Fig. 2), the response of the pier is strongly nonlinear with clear hysteretic loops in the $\{M_p - \kappa\}$ diagram. On the other hand, the dissipation in the foundation is very limited and only uplift mechanism is activated (notice the characteristic S-shaped $M_f - \theta_Z$ diagram) together with a slight accumulation of approximately 1.2cm of settlement. The consideration of surface waves significantly accentuates the distress in the pier leading to strong residual structural drift and high ductility demands. This increase in distress is however almost entirely due to the horizontal component of the surface waves (note that diagrams in columns 2 and 3 are almost identical).

For p21-RF (*cf.* Fig. 3), the reduction of foundation dimension concentrates all the nonlinearity at the foundation level while the pier remains elastic. The price to pay for this "isolation" effect is a high foundation

settlement and residual drift due residual foundation rotation. Notice the clear hysteretic loops at the $M_f - \theta_z$ diagram highlighting the dissipation at the foundation. This behavior is aligned with the observations and suggestions by Anastasopoulos *et al.* [8] for exploiting soil nonlinear behavior in seismic protection of structures. However, when the surface wave effect is considered, the distress in the foundation is strongly accentuated and the foundation settlement is almost doubled (passing from 16cm to 32cm). As in the previous case, this additional distress is almost exclusively due to the horizontal surface wave component.

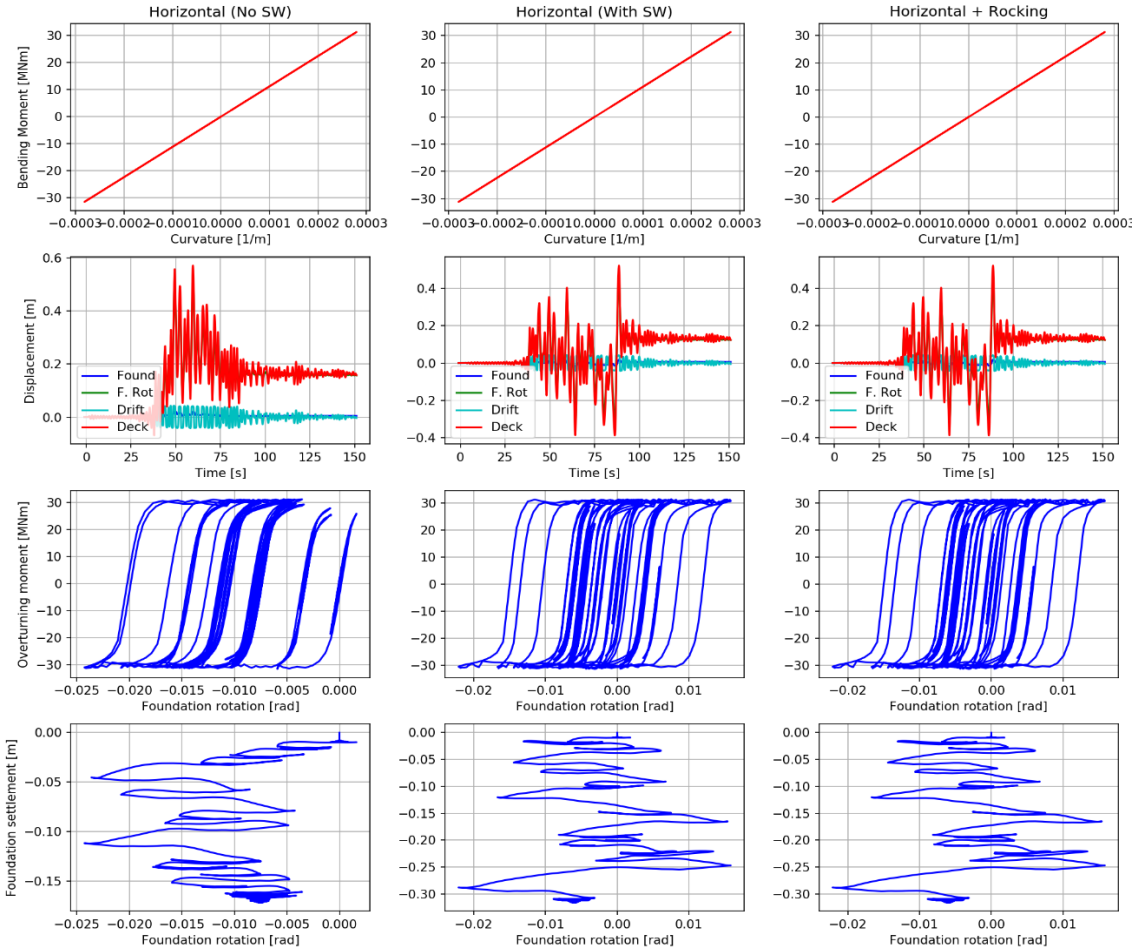

Fig. 3 – Response of p21-RF for record TCU140

5.2 Radar plots for performance criteria

A more synthetic appraisal of the dynamic response can be obtained by examining some characteristic performance criteria that can be defined with the aid of diagrams of Figs. 2 and 3. For the present study, we choose 7 performance criteria, namely:

1. The maximum total drift (MTD) of the deck
2. The maximum structural drift (MSD) of the deck, *i.e.* the displacement component exclusively due to the pier deformation
3. The residual total drift (RTD) of the deck
4. The residual structural drift (RSD) of the deck: this quantity can be high if the pier response is strongly nonlinear
5. The maximum ductility demand (DD) obtained at the base of the pylon
6. The accumulated foundation settlement (FS) at the end of loading
7. The maximum moment (MM) developed at the base of the pier

These performance criteria are plotted in radar diagrams for each studied case. Each radar diagram contains three curves corresponding to the three considered excitation scenarios (blue curve: Horizontal, no SW / red curve: Horizontal, with SW / green curve: Horizontal and Rocking, with SW). Fig. 4 presents the radar plots for p21 and p30 together with the configurations p21-RF and p30-RF. Fig. 5 provides the radar plots for configurations p40, p50 and p60.

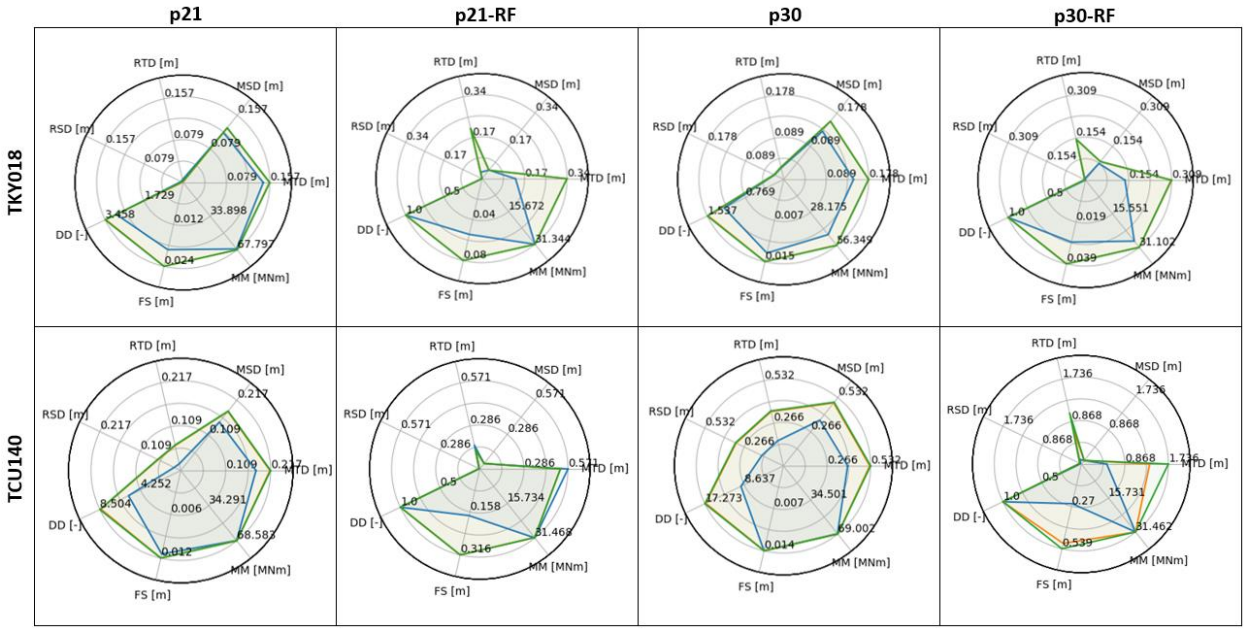

Fig. 4 – Performance criteria in radar plots - Comparison for piers with basic and reduced foundation
Blue curve: Scenario 1 / Red curve: Scenario 2 / Green curve: Scenario 3

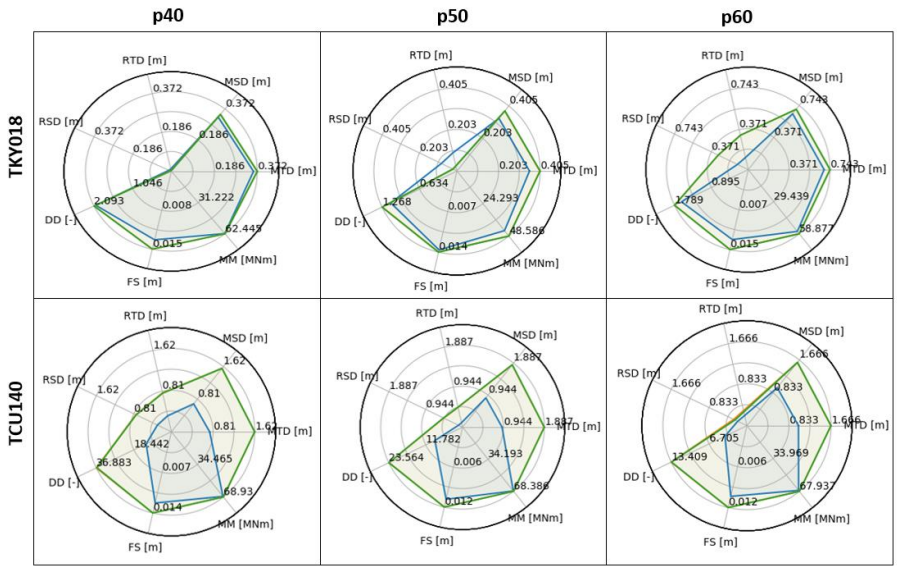

Fig. 5 – Performance criteria in radar plots - Comparison for piers p40, p50 and p60
Blue curve: Scenario 1 / Green curve: Scenario 2 / Red curve: Scenario 3

The radar diagrams allow for an immediate quantification of the variation of any performance criterion when the surface wave effect is considered. It is interesting to notice that the green and red curves are almost superposed for all the studied cases, which means that the SW effect is predominantly obtained from the

horizontal component. In the considered records, the rotational component is rather low and has a negligible impact on the studied structures (the only exception is case p30-RF under TCU140. This is a situation with very strong nonlinear response at the foundation, with settlements exceeding 50cm and total drifts reaching almost 1.8m). However, the horizontal component of surface waves may lead to severe amplifications in all studied performance criteria and independently of the adopted strategy for seismic design (conventional or reduced foundation). In particular, an increase by a factor 2 is obtained for foundation settlement for p21-RF and p30-RF. The maximum increase in ductility demand is around 4, for cases p40 and p60 under TCU140. Maximal and residual drifts can be increased by a factor 2 to 4 as in piers p30-RF and p60 under TCU140.

7. Conclusions and perspectives

The present work aimed at a preliminary investigation of the effect of surface waves on the nonlinear seismic response of bridge pylons. To this end, a concise surrogate model has been proposed based on a multi-fiber model for the bridge pier and a nonlinear macroelement for the foundation. Despite its simplicity, the model retains the basic features of nonlinear pier response that, according to the designer's decision, can be mainly placed either on the pier or on the foundation. The surrogate model has been used for studying several configurations under excitations that preserve or not the horizontal and rotational surface wave component. The results have been organized based on performance criteria and radar diagrams that allow for an easy quantification of the increase in demand due to surface waves.

Following the presented preliminary results, it is intended to use the proposed surrogate model and analysis methodology in further parametric analyses for studying the influence of several parameters ($P-\Delta$ effect, excitation characteristics, pier properties *etc*.) on the response and for identifying the bridge pylon configurations that are more vulnerable to the effect of surface waves.

7. Acknowledgements

This research work has received funding from the French National Research project ANR MODULATE.

8. References

[1] Meza Fajardo KC, Papageorgiou AS (2018): Response of tall buildings to base rocking induced by Rayleigh waves. *Earthquake Engineering & Structural Dynamics*, 2018; 47:1755-1773, https://doi.org/10.1002/eqe.3040.

[2] Meza Fajardo KC, Papageorgiou AS (2019): Ductility demands of tall buildings subjected to base rocking induced by Rayleigh waves. *Earthquake Engineering & Structural Dynamics*, 2019; 1-21, https://doi.org/10.1002/eqe.3179.

[3] Chatzigogos CT, Figini R, Pecker A, Salençon J (2011): A macroelement formulation for shallow foundations on cohesive and frictional soil. *International Journal for Numerical and Analytical Methods in Geomechanics*, 2011; 35: 902-931

[4] Code_ASTER - Analyse des Structures et Thermo-Mécanique pour des Etudes et des Recherches (https://www.code-aster.org)

[5] Gazetas G (1991) - Foundation vibrations. In *Foundation Engineering Handbook*, Chapter 15, Fang HY(ed.), Van Nostrand Reinhold, NY.

[6] Dafalias YF, Hermann LR (1982) - Bounding surface formulation of soil plasticity. In *Soil Mechanics - transient and cyclic loading*, Pande GN, Zienkiewicz PC (eds.), Wiley, pp. 173-218.

[7] Chatzigogos CT, Pecker A (2009) - Project DARE - *Soil-Foundation-Structure systems beyond conventional seismic failure thresholds*, GDS Internal report 32-09_N1A.

[8] Anastasopoulos I, Gazetas G, Loli M, Apostolou M, Gerolymos N (2010) - Soil failure can be used for seismic protections of structures. *Bulletin of Earthquake Engineering*, 8:309-326

